Pergamon

Int. J. Heat Mass Transfer. Vol. 40, No. 8, pp. 1875–1884, 1997

0017–9310/97 $17.00 + 0.00

PII: S0017–9310(96)00218–9

Modelling the behaviour of stratified liquid natural gas in storage tanks: a study of the rollover phenomenon

S. BATES† and D. S. MORRISON‡

British Gas, Gas Research Centre, Ashby Road, Loughborough LE11 3QU, U.K.

(*Received* 12 *April* 1995 *and in final form* 20 *June* 1996)

Abstract—The evolution of stratified liquid natural gas (LNG), from its formation to its breakdown, is considered. Experimental observations have shown this evolution to consist of two principle phases: a quiescent, stable phase 1 where the interface between the two layers is stationary; and an unstable phase 2 characterised by a migrating interface and culminating in a rollover. Mathematical models of the two phases are proposed and considered separately. For phase 1 a parametric solution is derived; the corresponding numerical solution of phase 2 equations is given and shown to compare well with experimental data.

1. INTRODUCTION

The capacity of liquid natural gas (LNG) for yielding large volumes of gas (a ratio of $\approx 600:1$ at STP) has made it an important component in the modern gas supply industry. When not in transit LNG is stored in large holding tanks (up to 200 000 m^3 in volume) until required for release into the transmission system. These tanks are normally located at importation terminals or at so called 'peak shaving' sites. The former constitute an essential link in the supply chain; the LNG turnover at terminals is necessarily high. The latter act as security against extreme conditions like cold weather or pipeline failure; in this case turnover can be negligible over a period of months or years. For both sites, however, the tank maintenance procedures remain the same.

Typically, the LNG resides within the tank at temperatures just below boiling (≈ 120 K) and at a *gauge* pressure of 150.0 mbar. The tanks are heavily insulated with fibre glass and perlite. The heat flux, which can be as small as 4 W m^{-2} for some tanks, is absorbed by the LNG and ultimately converted into vapour evolution. By this mechanism a 60 000 m^3 tank containing 25 000 tonnes of LNG will lose an *average* of 12.5 tonnes per day through vaporisation while maintaining a constant, *average* temperature (at least over a period of months). The emphasis on '*average*' is made because the tanks often operate under gauge pressure. Hence, barometric highs increase *absolute* vapour space pressure and suppress evaporation; barometric lows have the reverse effect. Extreme conditions are alleviated by the use of compressors which remove vapour build up.

During its residence within a tank, LNG will slowly change in composition as its components vaporise at different rates. Methane, which usually comprises over 90% of the mixture, is removed at a faster rate than the heavier hydrocarbons like ethane and propane. The result of this 'weathering' is to effectively increase the density of the LNG as well as marginally changing the temperature at which evaporation preferentially occurs. After a long period of storage, which may be years in the case of a peak shaving site, the residual LNG is warmer and denser than the original product. This has important consequences when fresh LNG is added to the tank.

An unavoidable practice on LNG sites is the mixing of two different products in the same tank. This could occur, for example, at import terminals when supply does not match demand. Inevitably, the new stock (the cargo) is lighter and cooler than the old (the heel) which has had time to weather during its period in the tank. If precautionary measures fail, the LNG stratifies into two distinct layers with the warmer 'heel' lying below the cooler 'cargo' as idealised in Fig. 1. Between the two an apparently stable interface restricts the transfer of heat and mass from the lower layer to the upper surface; heat absorbed by the heel partly accumulates there. Eventually, the thermal expansion of the heel reduces its density to the extent that the interface destabilises (this process is enhanced by the flux of *heavier* components from the heel to the cargo). The ultimate breakdown of stratification results in the sudden release of the heat trapped in the lower layer and an attendant increase in vapour evolution rates. This phenomenon is sufficiently common in site operations to be identified as an 'LNG rollover', examples of which are documented in ref. [1].

In terms of density and temperature profiles roll-

†Present address: Edinburgh Petroleum Services, Research Park, Riccarton, Edinburgh EH14 4AP, U.K.

‡Present address: School of Engineering, Durham University, Durham, U.K.

NOMENCLATURE

A	cross sectional area
C_p	molar specific heat
C_0	correction factor in temperature entrainment formula
H	heat leak into the layer through the tank walls
Hf	heat flux into the layer through the tank walls
h	coefficient of heat diffusion
h_l	lower layer depth
h_u	upper layer depth
K	constant of proportionality in entrainment formula
k	coefficient of mass diffusion
Lh	latent heat of vaporisation
M	total mass of a layer
Mol	molar mass of layer
m	mass of component in a layer
m_j	coefficients in molar mass expansion
t	time
R	stability number
Rc	critical stability number
S_b	amount of heat required for boil-off
S	mass fraction. Thus, S^i = (mass) fraction of component i in a layer
T	temperature above some reference level
T_j	coefficient in temperature expansion
u	interface speed
V_i	molar fraction of component 'i' ($i = 1, 5$) that boils off
x_i	molar fraction of component 'i' in lower layer ($i = 1, 5$)
x_j^i	coefficients in molar fraction expansion
y_i	molar fraction of component 'i' in upper layer ($i = 1, 5$)
y_j^i	coefficients in molar fraction expansion.

Greek symbols

α	$(1/\rho)\,\partial\rho/\partial S$
β	$-(1/\rho)\,\partial\rho/\partial T$
δ	changes in a layer over a period of time e.g. δT temperature change
Δ	differences across an interface e.g. $\Delta T = T_u - T_l$
ρ	density.

Subscript

c	correction factor
i	component i
in	interface
j	coefficient expansion
l	lower layer
u	upper layer.

Superscripts

i	component i.

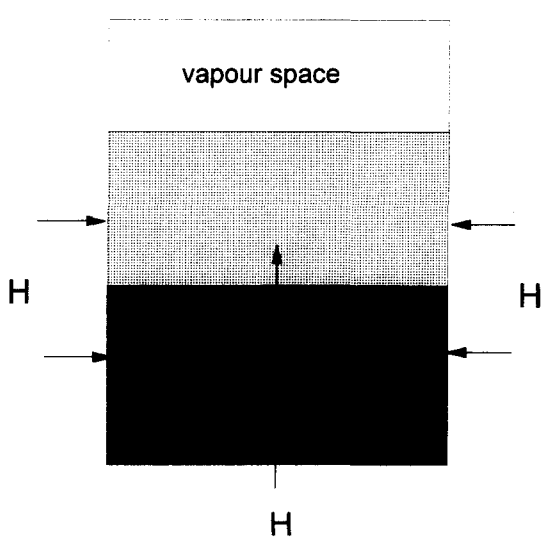

Fig. 1. Schematic of stratified LNG showing directions of heat flow through the liquid. H is the heat leak into the tank; h, k are the coefficients of heat and mass transfer that govern exchanges across the interface.

over is characterised by the profiles of Fig. 2 showing the densities of two layers equalising when a temperature jump exists across the interface. The final value of the interfacial temperature difference depends on many factors like initial layer temperatures and compositions, and can vary enormously. Its determination is crucial to the prediction of rollover discharge rates which can vary from a barely perceptible rise in tank pressure to a surge that necessitates emergency venting of excess gas to the atmosphere.

For a long time industrial users have been conscious of the need to protect their sites against LNG rollover. The widely reported incident at La Spezia, Italy [2] in 1971, and the concurrent availability of high speed computers gave impetus to the formulation of practical models. The early models of Chatterjee and Geist [3] and Germeles [4] were later refined and implemented by Heestand, Shipman and Meader [5] (HSM) into the Cabot Corporation ROLLO program. For given initial temperatures and compositions, ROLLO computes the evolution of stratified LNG by numerically solving the appropriate

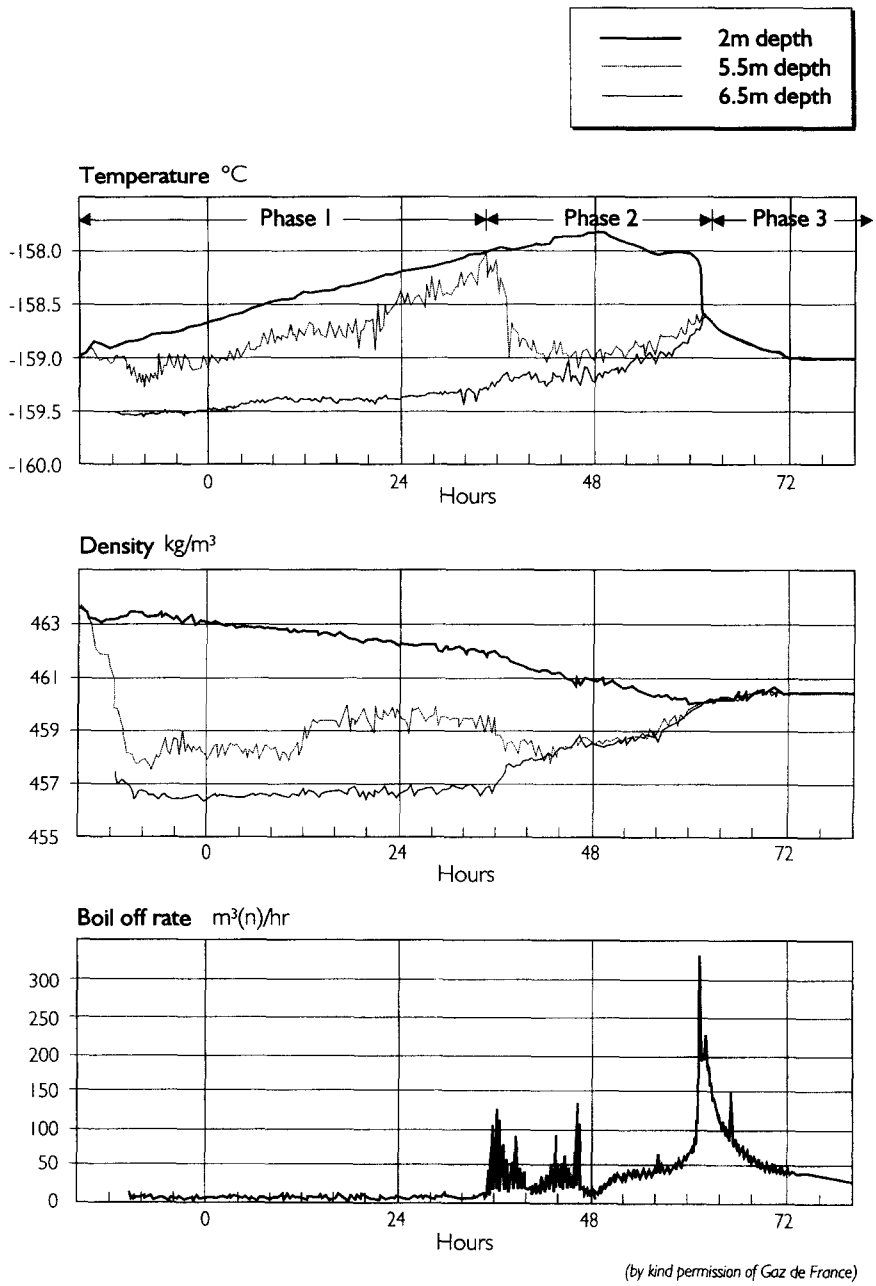

Fig. 2. LNG experimental results.

(temporal) differential equations ((1) to (7)). The interface between layers is defined as *stationary* and the interfacial fluxes obtained from sources such as Turner's [6] double diffusive correlations for heat–salt solutions.

At about the same time British Gas Research and Technology undertook a series of experiments with liquid petroleum gas (LPG) which provided a good qualitative description of how stratifications evolve with time [7]. In brief, the results confirmed an initially stationary interface with small heat/mass exchanges between the layers—akin to double diffusive convection. However, later stages of each experiment were dominated by an interface migration that had not been anticipated by the earlier models. Further comparison with the publication of Kamiya *et al.* [8], for large scale LNG tanks, and with the commercially available LNG data of Gaz de France [9], confirmed the British Gas findings. Clearly the need had arisen for a more detailed analysis of stratified LNG behaviour. This paper is a summary of the analysis. In Section 2 HSM, which is still considered appropriate during the *early* stages of stratification, is re-examined. Sections 3 and 4 take a closer look at the effects of entrainment on densities/temperatures either side of a migrating interface during the *later* stages of stratification. The transition point between the two phases, quantifying '*early*' and '*later*', is usually

defined in terms of an empirical correlation which is a variation of $R = \alpha\Delta S/\beta\Delta T = 2$ for the heat/salt experiments of Turner [6]. For the purpose of the following theory the actual definition of the transition point correlation is ignored and the two phases are examined separately. Section 5 then briefly outlines applications of rollover models and Section 6 concludes.

2. PHASE 1 OF STRATIFICATION: STATIONARY INTERFACE

2.1. *Governing equations: formulation*

The one-dimensional HSM model solves for temperature and composition in each of the two LNG layers as a function of time. The source terms derive from the heat leak through the walls, the vapour release from the free surface and the exchange rates (heat and mass) at the interface. Compositions are defined by the molar fractions of the LNG components which we take to number five: methane, ethane, propane, butane and nitrogen. In their simplest form, with interfacial fluxes modelled by diffusion expressions, the HSM equations are summarised thus:

Lower layer. Mass diffusion:

$$\mathrm{d}(Mol_\mathrm{l} \cdot x_i)/\mathrm{d}t = k \cdot A \cdot (y_i - x_i). \tag{1}$$

Heat diffusion:

$$\mathrm{d}(Mol_\mathrm{l} \cdot C_\mathrm{pl} \cdot T_\mathrm{l})/\mathrm{d}t = h \cdot A \cdot \Delta T + H_\mathrm{l} + S_\mathrm{l} \tag{2}$$

where

$$S_\mathrm{l} = \sum_{i=1}^{i=5} (C_\mathrm{pl} T)\, \mathrm{d}(Mol_\mathrm{l} \cdot x_i)/\mathrm{d}t \tag{3}$$

and T is defined as T_u, if $(y_i - x_i)$ is positive and T_l if $(y_i - x_i)$ is negative. This models the transfer of heat into and out of the lower layer by mass diffusion. H_l is the wall heat leak into the lower layer which is typically measured in Watts.

Sum of molar fractions:

$$\sum_{i=1}^{i=5} x_i = 1. \tag{4}$$

Upper layer. Mass diffusion:

$$\mathrm{d}(Mol_\mathrm{u} \cdot y_i)/\mathrm{d}t = -k \cdot A \cdot (y_i - x_i) + V_i \cdot \mathrm{d}(Mol_\mathrm{u})/\mathrm{d}t. \tag{5}$$

Heat diffusion:

$$\mathrm{d}(Mol_\mathrm{u} \cdot C_\mathrm{pu} \cdot T_\mathrm{u})/\mathrm{d}t = -h \cdot A \cdot \Delta T + H_\mathrm{u} - S_\mathrm{l} + S_\mathrm{b}. \tag{6}$$

Sum of molar fractions:

$$\sum_{i=1}^{i=5} y_i = 1. \tag{7}$$

A justifiable expedient for solving the above equations is to assume that the upper layer temperature remains close to its bubble point at all times. Then, for a given composition and pressure both V_i and T_u may be computed from thermodynamics routines and equation (6) effectively eliminated. The justification derives from the fact that under normal operating conditions heat leak into the tank is converted directly into latent heat of vaporisation. This implies an approximate vapour–liquid equilibrium at the LNG surface; the bubble point calculation can then follow.

A further benefit arising from the bubble point assumption is that T_u varies slowly on a timescale defined by lower layer changes. Over short periods of time therefore (such as a day) equation (6) can be replaced by $T_\mathrm{u} = \text{const.}$ where the constant is updated at the end of each period. For gauge pressure tanks, of course, the changes in T_u will be superimposed on those due to barometric variations which would not be known in advance. However, the barometric temperature swings will have a zero mean and an amplitude typically much less than the extreme value of 0.4 K—a small fraction of the temperature difference existing across an interface. Hence, for the purpose of the present study, they are ignored.

Accepting $T_\mathrm{u} = \text{const.}$ as a reasonable approximation over a reduced timescale, equations (1)–(7) become:

Mass diffusion:

$$\mathrm{d}(Mol_\mathrm{l})/\mathrm{d}t = 0 \tag{8}$$

$$\mathrm{d}(Mol_\mathrm{l} \cdot x_i)/\mathrm{d}t = k \cdot A \cdot (y_i - x_i) \tag{9}$$

$$\mathrm{d}(Mol_\mathrm{u} \cdot y_i) = -k \cdot A \cdot (y_i - x_i) + V_i \cdot \mathrm{d}(Mol_\mathrm{u})/\mathrm{d}t. \tag{10}$$

Equation (8) is derived from equation (1) by summing over the five components and applying equations (4) and (7).

Heat diffusion:

$$S_\mathrm{v} \cdot \mathrm{d}(Mol_\mathrm{u})/\mathrm{d}t = -(H_\mathrm{l} + H_\mathrm{u}) + Mol_\mathrm{l} \cdot C_\mathrm{pl} \cdot \mathrm{d}(T_\mathrm{l} - T_\mathrm{u})/\mathrm{d}t \tag{11}$$

$$Mol_\mathrm{l} \cdot C_\mathrm{pl} \cdot \mathrm{d}(T_\mathrm{l} - T_\mathrm{u})/\mathrm{d}t = h \cdot A \cdot \Delta T + H_\mathrm{l} + S_\mathrm{l}. \tag{12}$$

S_v is defined by

$$S_\mathrm{v} = \sum_{i=1}^{i=5} V_i \cdot (Lh_i) \cdot mwt_i \tag{13}$$

and S_l by

$$S_\mathrm{l} = \sum_{i=1}^{i=5} Mol_\mathrm{l} \cdot C_\mathrm{pl} \cdot (T_\mathrm{l} - T_\mathrm{u}) \cdot \mathrm{d}(x_i)/\mathrm{d}t \tag{14}$$

where Lh_i is the latent heat and mwt_i the molecular weight of component 'i'. Note that in this version of the equations the constant T_u has been adopted as the reference temperature; as a result the $i = 1$ term in equation (14), which represents the transfer of heat

by methane diffusion from the top layer, reduces to zero. Equations (9) and (10) are solved for $i = 1, 5$ or alternatively $i = 1, 4$ with equations (4) and (7). Also, to simplify the solution procedure below, C_{pl}, the molar specific heat, is defined as constant. The small gain in accuracy from using variable C_{pl} ($\approx .1\%$) does not merit the extra effort required to include it in the solution procedure.

Equations (8), (9), (10) and (12) follow directly from equations (1)–(7) above. Equation (11) can be derived by summing the quantities of heat required to vaporise the individual components and then equating the sum with the *total* heat leak into the tank minus the heat warming up the lower layer. A correction factor can be introduced to account for the small temperature rise in the upper layer as recorded in the preceding time interval. Equation (11) implicitly assumes that the heat leak into the vapour space is transmitted directly to the upper layer and its effect included in H_u.

Equations (8)–(12) are now in a closed form: effectively 13 equations for the 13 unknowns x_i, y_i ($i = 1, 5$), T_l, Mol_l, Mol_u. Site data can provide values for all the relevant parameters except 'h' and 'k' which are normally defined by empirical correlations. In the HSM model the equivalent equations are solved numerically using a time-marching Runge–Kutta scheme. For equations (8)–(12), however, a direct series solution is possible.

2.2. *Governing equations: validity and solution*

An assumption inherent to the governing equations is that of a stationary interface. For stable layers coupled by double diffusive convection the existence of a stationary interface is well documented both for LNG [10] and LPG [7]. However, the stability of stratified LNG is continuously being eroded by the accumulation of heat in the lower layer and the accumulation of concentrates in the upper. Eventually, the interfacial density difference will be reduced to a point where it is unable to resist the convective motions in one or both of the layers. From then on, the predominating exchange mechanism at the interface will be 'penetrative convection', a description of the process whereby plumes of liquid from one layer penetrate the interface, entrain fluid from the other layer and then return under their own buoyancy [6, 11, 12]. The plumes are unsteady and with a high Rayleigh Number $O(10^{10})$, necessarily turbulent. Their dynamics contrasts in detail, if not in effect, with the laminar model of entrainment proposed by Shi *et al.* [13]. This effect, as described in refs. [7, 8, 13], is a migration of the interface, up or down, culminating in density equalisation and rollover. In their present form equations (8)–(12) would not then be applicable although simple modifications that effectively account for interface movement can be made.

A more direct approach to modelling the entrainment regime is described in the next section. Before then we set out the solution details of equations (8)–(12) that apply strictly to a stationary interface. It should be emphasised here that the time elapsing before the interface starts to migrate is often an order of magnitude longer than the period of migration itself [7]. An interface that migrates immediately after formation is intrinsically unstable and characterised by a low Stability Number (defined in ref. [6] as $R = \alpha\Delta S/\beta\Delta T$). Examples of this are given in Kamiya *et al.* [7]; also, La Spezia [2] with its very low initial stability number (≈ 6) is probably another example of rapid mixing due to entrainment although no density profiles were recorded to prove this conjecture. In general however, the entrainment phase is preceded by a lengthy period when double diffusive convection alone acts at the interface. It is very important, therefore, that this initial phase is simulated correctly for an accurate prediction of time to rollover.

The linear form of equations (8)–(12) suggests a series solution that proceeds in integral powers. Assuming 'h' and 'k' are constant, at least over the reduced time interval described above, the relevant expansions are:

$$x_i = \sum_{j=0}^{j=\infty} x_j^i t^j \tag{15}$$

($i = 1, 5$)

$$y_i = \sum_{j=0}^{j=\infty} y_j^i t^j \tag{16}$$

($i = 1, 5$)

$$Mol_u = \sum_{j=0}^{j=\infty} m_j t^j \tag{17}$$

$$T_l - T_u = \sum_{j=0}^{j=\infty} T_j t^j. \tag{18}$$

The constants x_j^i, y_j^i, m_j, T_j are determined by the differential equations and their initial conditions x_0^i, y_0^i, m_0, T_0. If the expansions are substituted into equations (9)–(12) in the order (9), (12), (11), (10), and the coefficients of powers of 't' equated, the following recurrence formulae are obtained:

$$x_n^i = k \cdot A \cdot (y_{n-1}^i - x_{n-1}^i)/(n \cdot Mol_l) \tag{19}$$

$$T_n = (-h \cdot A \cdot T_{n-1} + g(n) \cdot H_l + S_{nl})/(n \cdot Mol_l \cdot C_{pl}) \tag{20}$$

where $g(n) = 1$ for $n = 1$, $g(n) = 0$ otherwise and

$$S_{nl} = Mol_l \cdot C_{pl} \cdot \sum_{i=2}^{i=5} \cdot \sum_{j=0}^{j=n-1} T_j \cdot (n-j) \cdot x_{n-j}^i \tag{21}$$

$$m_n = (-g(n) \cdot (H_l + H_u) + Mol_l \cdot C_{pl} \cdot T_n)/S_v \tag{22}$$

$$y_n^i = (-k \cdot A \cdot (y_{n-1}^i - x_{n-1}^i) + V_i \cdot n \cdot m_n - S_1 - S_2)/n \cdot m_0 \tag{23}$$

where

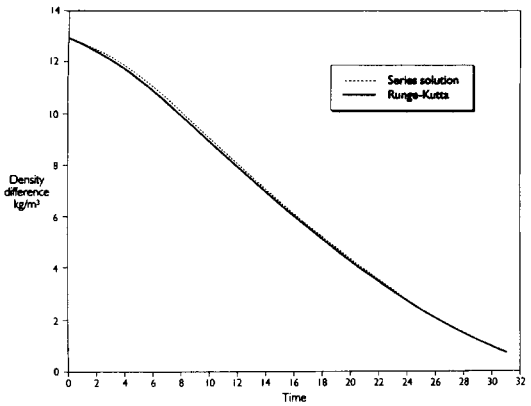

Fig. 3. A typical variation of interfacial density difference with time.

$$S_1 = \sum_{j=0}^{j=n-1} y_j^i \cdot (n-j) \cdot m_{n-j} \tag{24}$$

$$S_2 = \sum_{j=0}^{j=n-1} m_j \cdot (n-j) \cdot y_{n-j}^i. \tag{25}$$

The computation of the expansion coefficients is straightforward; no more than 20 terms in each series are needed to guarantee accuracy. Substitution back into equations (15)–(18) gives the temperature and composition for both layers at any time. The densities can then be derived from standard thermodynamical formulae. The analysis assumes constant h, k, T_u over the reduced time interval. For integrations over longer timespans h, k, T_u must be updated periodically using empirical and thermodynamics routines. Within the context of the entire integration h, k, T_u are hence being modelled by piecewise-constant functions. In programming terms this entails re-computing the series coefficients at the beginning of each interval with initial conditions derived from the end of the previous interval. The extra coding involved is minimal. Fig. 3 shows a direct comparison between the series solution and the more elaborate Runge–Kutta scheme for transfer coefficients proportional to $\Delta T^{1/3}$. Runge–Kutta was applied for a time step of 0.04 units guaranteeing an accuracy of $O(10^{-7})$ in the density profile. Re-computing the series coefficients 30 times in the entire timespan gives very good agreement between the two schemes.

A useful exercise at this point is to assess the relative importance of the input parameters on the duration of phase 1. For a given stratification, the changes through phase 1 will be strongly influenced by h, k the interfacial transfer constants and Hf the heat flux through the tank walls. In the absence of any conflicting evidence, it seems reasonable to vary h, k according to Turner's [6] findings for heat–salt solutions; hence the ratio of the density fluxes across the interface is held at 0.15 (the justification of this constraint is that the same molecular process of diffusion dictates the transfer rates in both cases). The wall heat flux (Hf) for British Gas peak shaving sites is typically 4 W m^{-2}.

The development of a stratification in a peak shaving tank was simulated for a given Hf (4 W m^{-2}), for constant density flux ratios (0.15), and for a different interfacial heat transfer rate in each case. Each simulation was terminated when the stability number R had descended to a pre-determined, critical value (Rc); the time to the end of phase 1 was then recorded. It was found that increasing the interfacial heat flux from 0.1 to 2.0 W m^{-2} ($\approx$2000%) extended the duration of phase 1 by the much smaller margin of 16%. The opposing effects of heat and mass transfer at the interface are evidently rendering the *precise* values of h, k unimportant. Unfortunately, the same does not appear to be true for the critical stability number Rc (marking the end of phase 1); typically, a 50% variation in Rc implies a 25% variation in phase 1 duration. Hence, the predictions of a rollover model depend much more sensitively on the value of Rc than on the values of h, k.

To conclude then: the series solution is an extremely simple method for computing how long a given stratification will persist before reaching some pre-determined, critical value. For an accurate prediction, more emphasis must be placed on evaluating the critical point stability number (Rc) than on the interfacial transfer parameters (h, k). The evolution beyond the critical point, when entrainment prevails, is examined in the next section.

3. STAGE 2 OF STRATIFICATION: MIGRATING INTERFACE

A reliable definition of the parameters: (a) when entrainments begins; (b) the rate of entrainment for a given stratification, would require access to high quality commercial data. Indeed, correlations for (b) are further dependent on boundary layer formulae when velocity measurements are not available (see, e.g. ref. [8]). For the present purposes we assume that both (a) and (b) have been adequately defined empirically and proceed to derive results in a parametric form. In Section 4 a comparison is made between theory and experiment.

3.1. *Analysis of penetrative convection*

Penetrative convection has been described (Section 2) as plumes in one layer entraining fluid from another and returning under their own buoyancy. As fluid is removed from one layer the interface between the two will move perceptibly and their relative densities will decrease. It is important to realise that mixing can take place in both directions simultaneously with the interface moving away from the more energetic of the two regions. The whole process is, therefore, quite a vigorous and efficient means of undermining the density/temperature differences between layers. Furthermore, its simple physics—small portions from one region being removed bodily to the other—allows a

linear analysis to be performed that leads to useful results.

Considering, firstly, liquid being entrained from the upper layer into the lower. If m^i denotes the mass of component 'i' in a layer, M the total mass, and S^i the corresponding mass fraction, then (for the lower layer):

$$S_l^i = m_l^i / M_l. \tag{26}$$

If a small quantity of fluid, δM_u, is entrained from the upper layer this process can be represented mathematically by

$$S_l^i + \delta S_l^i = (m_l^i + \delta m_u^i)/(M_l + \delta M_u) \tag{27}$$

where δm_u^i is the amount of component i in δM_u. From equations (26) and (27) and linearising, we have (ignoring details of manipulation)

$$\delta S_l^i = (\delta M_u / M_l)(S_u^i - S_l^i). \tag{28}$$

Multiplying equation (28) by α_i and summing over all the components except methane ($i = 1$):

$$\sum_{i=2}^{i=5} \alpha_i \delta S_l^i = \sum_{i=2}^{i=5} \alpha_i (\delta M_u / M_l)(S_u^i - S_l^i). \tag{29}$$

The energy (i.e. heat) equivalent of equation (29) is (ignoring the difference in specific heats between the layers)

$$\delta T_l = (\delta M_u / M_l)\, \Delta T \tag{30}$$

where δ refers to changes within a layer and Δ to changes across the interface ($\Delta T = T_u - T_l$). From equations (29) and (30)

$$\sum_{i=2}^{i=5} \alpha_i \delta S_l^i / (\beta \delta T_l) = \sum_{i=2}^{i=5} \alpha_i \Delta S^i / (\beta \Delta T). \tag{31}$$

Now,

$$\sum_{i=2}^{i=5} \alpha_i \delta S_l^i = \delta \rho_l / \rho_l + \beta \delta T_l \tag{32}$$

and

$$\sum_{i=2}^{i=5} \alpha_i \Delta S^i = \Delta \rho / \rho_u + \beta \Delta T \tag{33}$$

to first order (i.e. ignoring the square of $\delta\rho/\rho$). The first component is not included because the sum of the five mass fractions is equal to one (cf. equation (4)): ρ is effectively a function of *four* mass fractions plus temperature. Equations (31)–(33) can be combined to give, in the limit:

$$\mathrm{d}(\rho_l)/\mathrm{d}T_l = (\rho_l / \rho_u)(\Delta \rho / \Delta T). \tag{34}$$

For an interface whose transfer process is dominated by entrainment from *the upper layer only* T_u, ρ_u are effectively constant and equation (34) can be solved to give:

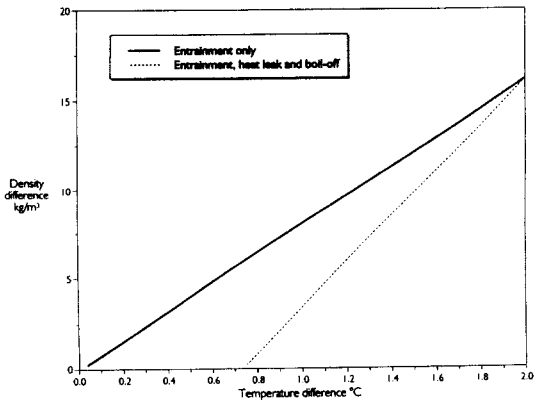

Fig. 4. An idealisation of how the density and temperature differences across an interface change with time due to convective entrainment. Line (i) (solid) represents entrainment alone. Line (ii) (dashed) is for entrainment modified by diffusive and boil-off effects.

$$\rho_u - \rho_l = K \rho_l (T_u - T_l) \tag{35}$$

or

$$\Delta \rho = K \rho_l \Delta T \tag{36}$$

where 'K' is a constant.

Equation (36) shows that temperature and density differences across an interface approach zero at the same time. The locus of $\Delta\rho$ against ΔT for arbitrary initial conditions and entrainment rates is a nearly straight line passing through the origin (Fig. 4, line (i)). If entrainment is in both directions simultaneously, then the same type of locus would be obtained, but no convenient formula like equation (34) is available to describe its exact shape. In either case the end-product of entrainment is to reduce the amount of superheat released when the densities finally equalise and a rollover occurs. The predominance of entrainment in the later stages of a stratification effectively reduces the final pressure peak.

In contrast the slower process of wall heat leak into the lower layer tends to drag the locus down towards the ΔT-axis and away from the origin i.e. in direct competition to entrainment (Fig. 4, line (ii)). So too, to a smaller extent, does the vapour release from the upper surface. Neither effect is accounted for by equation (34) which cannot, therefore, produce the more realistic locus. The next logical step is to combine the relevant processes into a useful, predictive formula.

3.2. *Computing the effects of penetrative convection*

An approximate method is now developed from equation (34) which can give quick and reliable predictions of the entrainment phase. In addition to the above notation, u_u is the speed with which the interface would move upwards when entrainment is from the upper layer only; u_l is the speed with which the interface would move downwards when entrainment is

from the lower layer only. The perceptible speed of the interface u_{in} is, hence, given by $u_{in} = u_u - u_l$.

Considering, firstly, a portion of fluid entrained from the upper layer into the lower in time δt equation (30) can be re-written:

$$\delta T_l = (\rho_u \cdot A \cdot u_u \cdot \delta t)\,\Delta T/M_l. \tag{37}$$

Combining this with equation (34) gives

$$\partial \rho_l/\partial t = u_u \cdot \Delta\rho/h_l. \tag{38}$$

As mentioned above, the density will also be changed during the time interval δt by the heat leak through the tank walls and the heat transfer through the interface. Equation (38), dealing with entrainment effects alone, must be changed accordingly. The simplest way of doing this is to include a correction term whose value equals the *$\partial\rho_l/\partial t$ computed during the first phase of the stratification.* Denoting the correction term by $\partial\rho_{lc}/\partial t$, equation (38) then becomes:

$$\partial \rho_l/\partial t = u_u \cdot \Delta\rho/h_l + \partial\rho_{lc}/\partial t. \tag{39}$$

The physical assumption underlying equation (39) is that the entrainment and the diffusive convection processes act independently of one another; in other words the inclusion of the extra term in (39) is an acknowledgement that the slower processes at play in stage 1 do not suddenly stop when entrainment begins. This agrees with an earlier study by Linden [14] on heat–salt systems.

Similar equations may be derived for the lower layer temperature and the upper layer density and temperature:

$$\partial T_l/\partial t = \Delta T(\rho_u/\rho_l)u_u/h_l + \partial T_{lc}/\partial t \tag{40}$$

$$\partial \rho_u/\partial t = -u_l\Delta\rho/h_u + \partial\rho_{uc}/\partial t \tag{41}$$

$$\partial T_u/\partial t = -\Delta T(\rho_l/\rho_u)u_l/h_u + \partial T_{uc}/\partial t \tag{42}$$

where subscript 'c' denotes the correction factors throughout. The main source of inaccuracy in equations (39)–(42) lies in equation (42) which does not reflect any translation of the upper layer heat gain into vapour release. In its present form equation (42) implies no increase of vapour release levels due to entrainment which is clearly at odds with the boil-off profile in Fig. 2. Some empirically derived correction factor is therefore required for the right hand side of equation (42). It is also true that the upper layer density, ρ_u, will increase as the lighter components vaporise, an effect not accounted for in equation (41). However, such an increase is quite small compared with the changes resulting from entrainment; some numerical estimates are given in the next section. In the meantime, if the boil-off effect on density is ignored but a correction factor, C_0, is introduced for temperature, equations (39)–(42) can be combined to give:

$$\partial(\rho_l - \rho_u)/\partial t = \Delta\rho(u_u/h_l + u_l/h_u) + \partial\rho_c/\partial t \tag{43}$$

$$\partial(T_l - T_u)/\partial t = \Delta T(u_u/h_l + C_0 u_l/h_u) + \partial T_c/\partial t \tag{44}$$

where $\rho_u/\rho_l \approx 1$ has been assumed (correct usually to within 2%). For a given set of parameters, equations (43) and (44) can be easily solved to produce a curve similar to (ii) in Fig. 4. It is also interesting to note that in the absence of correction factors, equations (43) and (44) are homogeneous and produce the curve (i) in Fig. 4 regardless of the u_u, u_l etc. values, thus agreeing with the simple model of entrainment.

4. RESULTS

Quantifying the parameters that appear in Sections 2 and 3 requires access to good quality experimental data [9]. An extract from ref. [9] is shown in Fig. 2 which shows densities, temperatures and boil-off rates plotted throughout the duration of a single experiment. The layer depths in this example were 5.5 m (lower layer) and 1.6 m (upper layer) and were formed in a 8.5 m × 8.5 m cylindrical, cryogenic tank by top-filling with the lighter product. After formation, the stratified liquid was maintained at constant gauge pressure and allowed to de-stabilise naturally without operator intervention. The different phases are well defined. In particular, note the 5.5 m profile (just below the initial interface) which for phase 1 has characteristics intermediate to the two layers before assuming the upper layer temperatures and densities as the interface moves down. The phase 1 trends can be reproduced by a computational model if 'h, k' (described in Section 2) are tuned accordingly. With enough experiments correlations relating 'h, k' to quantities like $\Delta\rho$, ΔT can be formulated. These can be used to predict the outcome of phase 1 of a stratification.

The dominant parameters of phase 2 (u_u, u_l), can be obtained from re-arranged equation (39):

$$u_u = (\partial\rho_l/\partial t - \partial\rho_{lc}/\partial t)(h_l/\Delta\rho) \tag{45}$$

and from the measurement of interface speed, u_{in}, where:

$$u_{in} = u_u - u_l. \tag{46}$$

Equations (45) and (46) should be compared with standard correlations for u_u, u_l to confirm their validity. Such correlations are usually expressed in terms of a Richardson number which, in turn, demands convective velocity measurements. In the absence of measured velocity profiles, empirical formulae for free convection next to a heated plate may be employed (as in ref. [8]) although the reliability of the formulae in this context is not known.

The formulae derived in Section 3 may, nevertheless, be partially confirmed using data for entrainment in *one* direction only. In Fig. 2, this occurs during the first 12 h of phase 2 and is recognisable by the following characteristics:

(1) Lower layer, phase 1 trends continue unchanged even though the interface has begun to migrate. The cooler liquid of the upper layer is *not*,

Table 1. Interface migration details for three tests

	Test 1	Test 2	Test 3
Density difference	21.4	15	5.6
Lower depth	2.6	3.2	5.5
Upper depth	0.65	1.7	1.6
Speed of interface	0.2	0.125	0.06
Correction factor	0.26	0.15	0.07

therefore, being entrained into the lower layer as a consequence of migration.

(2) A significant increase of boil-off rates is recorded, implying release of superheat from the lower layer.

Algebraically, entrainment in one direction is given by $u_u = 0$, $u_l = -u_{in}$. Equation (43) therefore predicts the interfacial density difference to vary according to:

$$\partial(\rho_l - \rho_u)/\partial t = \Delta\rho(u_l/h_u) + \partial\rho_c/\partial t. \qquad (47)$$

Taking u_l and $\partial\rho_c/\partial t$ (= rate of change of interfacial density difference during phase 1) directly from the experimental results defines the right hand side of equation (47) explicitly. If equation (47) is then solved numerically and its results compare favourably with the experiment's, then equation (43) is confirmed as a good model for the convective process. Three tests are considered; their initial conditions are shown in Table 1. SI units are used throughout (kg, m), but the unit of time is hours.

The comparison between experiment and theory is illustrated in Figs. 5–8. Tests 1 and 2 show good agreement; test 3 shows a noticeable deviation. The discrepancy in test 3 can be explained by the small density difference across the interface which is accentuated by the scale of the graph. Also, the density changes due to boil-off for the three tests are estimated as: 0.7, 0.3, 0.5 kg m^{-3}, respectively. These corrections improve the comparison of test 3 considerably without having a noticeable impact on the tests 1 and 2 graphs. The final figure, Fig. 8, shows the further effect of

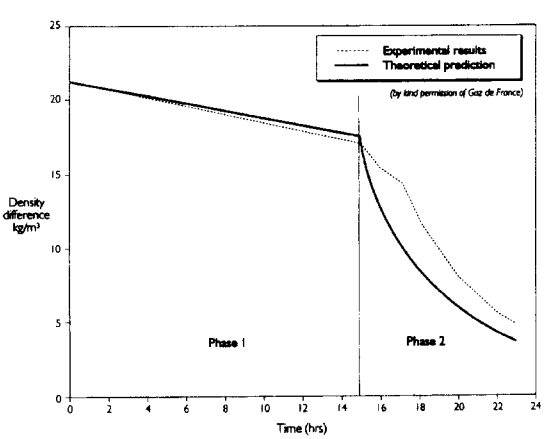

Fig. 5. Density difference across an interface (theory and experiment), test 1.

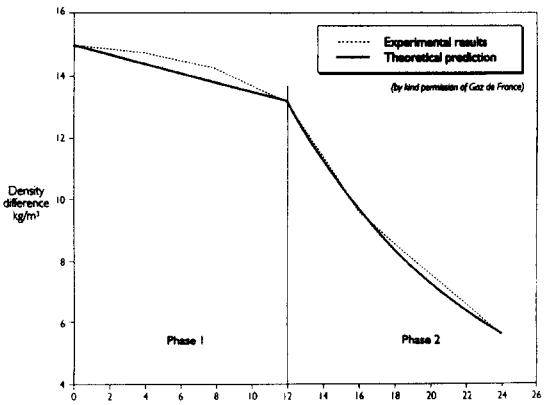

Fig. 6. Density difference across an interface (theory and experiment), test 2.

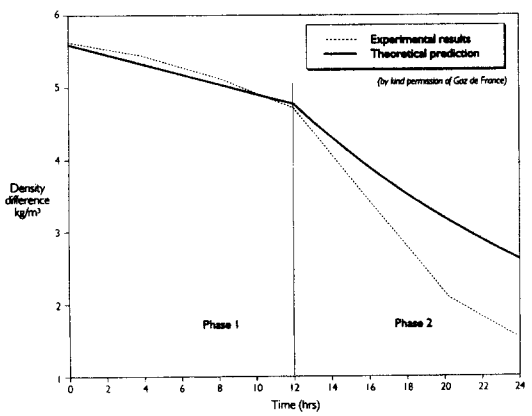

Fig. 7. Density difference across an interface (theory and experiment), test 3.

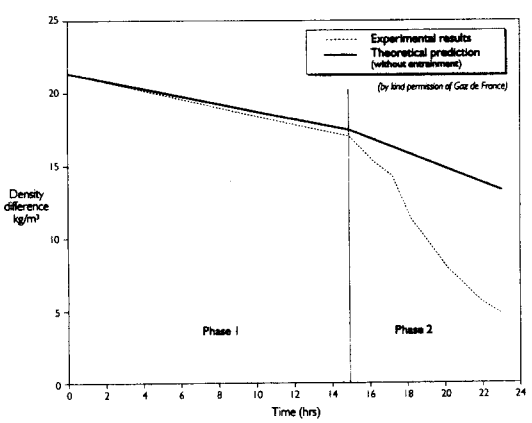

Fig. 8. Density difference across an interface (modified theory and experiment), test 1.

removing the entrainment contribution entirely while *doubling* that from double diffusive convection (i.e. putting $u_l = 0$, doubling $\partial\rho_c/\partial t$). It is clear from the figure that the sudden acceleration towards rollover is being driven by a much more efficient mechanism than double diffusive convection.

5. APPLICATIONS

The principle applications of a rollover model lie in the design of pressure relief valves (PRVs) and in

certain aspects of stock management. For example, there are suggestions from experimental and published data ([2, 9]) of a correlation between the accumulated heat in the lower layer and the resulting peak boil-off at rollover. It is therefore feasible to formulate a prediction of the most severe boil-off rate realisable under projected operating conditions, and use this information when specifying the design limits of PRV's on a new tank.

Again, a practice sometimes employed at import terminals is the deliberate formation of layers to reduce the amount of LNG lost to boil-off. Conventional LNG transfer from ship to shore can result in high boil-off rates as the cargo liquid adjusts to the equilibrium conditions of the tank vapour space. An alternative technique is to import the new product through a nozzle positioned near the bottom of the tank (bottom-fill procedure). Providing the cargo is denser than the heel, a stratification will form so that the new, denser product never comes into contact with the vapour space. It is then imperative that the time to rollover is computed and the lower layer exported before that time is reached. Predicted density/temperature profiles are usually compared against readings from an in-tank densitometer mast as a precautionary measure.

A further application exists in quantifying the hazards posed by projected layer formation, and planning accordingly. More stringent safety regulations are now demanding a clearer understanding of layer formation and evolution. In each of the above examples therefore, a carefully validated rollover model has an important role to play.

6. CONCLUSIONS

Early efforts to model LNG rollover were hampered by a lack of experimental data. Although conceptually sound, the models were ultimately driven by heat/mass flux correlations which had been obtained from related experiments and which, with the benefit of hindsight, were too simplistic. The stipulation, in particular, of a stationary interface was later found to be, at best, only partly true. Furthermore, in the absence of reliable data the models were validated by reproducing reported incidents like that at La Spezia [2]. The scarcity of measurements recorded during site incidents would not inspire much confidence in this form of validation. Clearly, a more systematic approach was required.

The first documented experiments with volatile mixtures revealed modes of behaviour not envisaged by the mathematical models. Kamiya *et al.* [8], working with a full scale LNG tank, showed interface migration to prevail in the period prior to rollover. Morrison [7], using LPG, and the LNG tests of Gaz de France *et al.* [9] not only repeated this result, but also showed how interface migration usually developed from a more stable phase typified by a stationary interface. In demonstrating consistently the evolution of stratified LNG these experiments provided a framework within which the different processes could be analysed.

The analyses set out in this paper were prompted by the experimental findings in ref. [9] and, in the case of entrainment, partly confirmed by them. For the stationary interface the model described is essentially the same as the early ones of refs. [3–5]. There is no reason why the model cannot be extended to account for interface migration but a numerical, time-marching solution would then be required. The alternative approach for interface migration (Section 3) provides insights to the entrainment process as well as a quick and easy solution procedure. Either way, implementation of the theory into a working computer model is straightforward; the difficulty will always lie in the reliable definition of the parameters, u_u, u_l, h, k in terms of the prevailing conditions.

Acknowledgements—The authors acknowledge access to the LNG experimental data [9]. They would also like to thank Paul Linden of DAMTP, Cambridge University and Olivier Marcel of Gaz de France for some useful discussions. The permission of The Cabot Corporation, U.S.A. to use their original ROLLO program is gratefully acknowledged.

REFERENCES

1. Acton, A. and Van Meerbeke, R. C., Rollover in LNG storage—an industry view. *LNG8 Conference*, LA, U.S.A., 1972, pp. 738–742.
2. Sarsten, J. A., *Pipeline Gas Journal*, 1972, **199**(11), 37–39.
3. Chatterjee, N. and Geist, J. M., *Pipeline Gas Journal*, 1972, **199**, 40–45.
4. Germeles, A. E., A model for LNG tank rollover. *Advances in Cryogenic Engineering*, 1975, **21**, 326–336.
5. Heestand, J., Shipman, C. W. and Meader J. W., A predictive model for rollover in stratified LNG tanks. *A.I.Ch.E. Journal* 1983, **29**(2), 199–207.
6. Turner, J. S., *Buoyancy Effects In Fluids*, Cambridge University Press, Cambridge, 1973.
7. Morrison, D. S. and Richardson, A., An experimental study on the stability of stratified layers and rollover in LNG storage tanks. *Proceedings of the Low Temperature Engineering and Cryogenics Conference*, Southampton, U.K. 1990.
8. Kamiya, A., Tahsita, M. and Sugawara, Y., An experimental study of LNG Rollover phenomenon. *Authority of Mtg. American Society of Mechanical Engineers*, New York, U.S.A. 1985, pp. 1–11.
9. Gaz de France, Shell Research Ltd, Osaka Gas, Tokyo Gas and CFP-Total, Experimental study of stratified LNG performed at Nantes Cryogenic Testing Station, 1987 to 1990.
10. Muro, M., Yoshiwa, M., Yasuda, Y., Miyata, T., Iwata, Y. and Yamazaki, Y., Experimental and analytical study of the rollover phenomenon using LNG. *ICEC* 11 *Conference*, Berlin, 1986, pp. 633–637.
11. Agabi, T., Rollover and interfacial studies in LNG mixtures. PhD Thesis, University of Southampton, Southampton, U.K., 1987.
12. Tasker, M. N., The effect of heat transfer on the dispersion of cold dense gases. Oxford University report OUEL 1688/87, 1988.
13. Shi, J. Q., Beduz, C. and Scurlock, R. G., Numerical modelling and flow visualisation of mixing of stratified layers and rollover in LNG. *Cryogenics*, 1993, **33**(12), 1116–1124.
14. Linden, P. F., A note on the transport across a diffusive interface. *Deep-Sea Research*, 1974, **21**, 283–287.